Research Journal of Chemical Sciences _____ ISSN 2231-606X
Vol. **3(7),** 62-68, July **(2013)** *Res. J. Chem. Sci.*

Generation of Hematite Nanoparticles via Sol-Gel Method

Samira Bagheri, Chandrappa K. G.* and Sharifah Bee Abd Hamid
Nanotechnology and Catalysis research centre (NANOCAT), IPS Building, University of Malaya, 50603 Kuala Lumpur, MALAYSIA

Available online at: www.isca.in
Received 17th June 2013, revised 27th June 2013, accepted 16th July 2013

Abstract

Nanocrystalline α-Fe_2O_3 (hematite) particles were successfully synthesized by sol-gel method using gelatin as a polymerizing agent. The main advantage of using gelatin is that it provides long-term stability for nanoparticles and by preventing the particles agglomeration. The precursor compound was calcined at a temperature of 600°C. The shape, size and chemical state of the synthesized powders were structurally characterized by TGA, SEM, TEM, powder XRD, FT-IR and UV–Vis spectral techniques. The thermal behavior of precursor compound was studied by using TGA results. Uniform spherical like morphology was confirmed by SEM photomicrographs and TEM result revealed the particle morphology was pseudo spherical in nature and particle sizes was around 30–40 nm. The UV–Visible spectrum was noticed the absorption and also the band gap is around 2.2 eV. The sol-gel synthesized α-Fe_2O_3 powder was simple, cost effective and eco-friendly in nature and also can be extended to prepare nanosized particles of other interesting materials.

Keywords: Hematite, Sol-gel, SEM, gelatin, spindle, spherical.

Introduction

Recently, nanostructured materials have received significant interests because of their unique optical, electronic, magnetic and physico-chemical properties that diverge greatly from their bulk materials. Nowadays tremendous amount of interest has been generated in the study of metal oxide materials because they lead to grow a new generation of optics, sensors, photocatalysis, electrocatalysis, anticorrosion, electronic and magnetic applications[1-3]. The oxides of transition metals like Zn, Cu, Ni, Ti, Sn, Fe, Co and W etc, have received an excellent properties in different areas like material science, chemistry and physics, which in turn have produced current exploitation and vast applications in magnetic devices, microelectronics, biomedicals, electrocatalysis, photocatalysis, anticorrosive coatings and powder metallurgy[4-9]. Among all oxides, iron oxide material including magnetite (Fe_3O_4) and hematite (α-Fe_2O_3) have attracted much attention due to their size, architecture, chemical, electrical, magnetic, anticorrosive and optical properties.

Iron oxide exists in number of different phases such as hematite (α-Fe_2O_3), magnetite (Fe_3O_4), akaganeite (β-Fe_2O_3) and maghemite (γ-Fe_2O_3). Among those phases, hematite (α-Fe_2O_3) is one of the most attractive and significant metal oxide[10], and it reveals the diverse configurations of nanostructures like tubes, wires, belts, cubes, rods, spindles, plates, rings, flowers, flakes, flutes, cups, hollow fibres, hollow microspheres, rhombohedra, quasicubic, shuttle, urchin-like and complex hierarchical structures constructed with nanoscale building blocks and ordered mesoporous α-Fe_2O_3[11-13]. Jiao and his co-workers[14] prepared ordered mesoporous α-Fe_2O_3 with crystalline walls through silica template; Tang and his co-workers[15] reported the synthesis of α-Fe_2O_3 nanorods through the calcination of FeOOH nanorods precursor; Chen and his co-workers[16] have prepared different morphologic α-Fe_2O_3 nanoparticles by solvothermal process. P. Deb and his co-workers[17] synthesized nanosized α-Fe_2O_3 nanoparticles by thermolysis; Zhao and his co-workers[18] have successfully synthesized monodisperse α-Fe_2O_3 by hydrothermal method; Xiong and his co-workers[19] described that the catalytic activity by decreasing the lowest complete CO conversion temperature could promote by hollow nanowires, and they attributed the improvement of catalytic activity to the hollow structures. Li and his co-workers[20] have reported that hematite nanocrystals by hydrothermal synthesis; Cao and his co-workers[21] have employed hydrothermal technique to prepare micropine structure of α-Fe_2O_3. The excellent catalytic activity of α-Fe_2O_3 might be allowed to replacing the CO oxidation by expensive precious-metal-containing catalysts. In spite of these applications, the size, morphology, agglomerated state and specific surface area of α-Fe_2O_3 nanoparticles are of great importance, and all of these features are strongly dependent on the preparation method. Thus, it is important to generate α-Fe_2O_3 with particular nanostructures that may broaden its application in different areas.

Currently, the hematite (α-Fe_2O_3) nanomaterial can be synthesized by different methods like sol–gel, microemulsion, forced hydrolysis, precipitation, polymerization, direct oxidation, thermal decomposition, sonochemical, hydrothermal, solvothermal, electrochemical[22], solution combustion, pyrolysis and gamma-irradiation techniques are reported. However, still it is a tackle to develop direct and facile methods for synthesizing α-Fe_2O_3 nanoparticles. In the present work, we focus on the synthesis of iron oxide (α-Fe_2O_3) nanoparticles by sol-gel route using gelatin as polymerizing agent in which it serves as terminator that terminates the growth of nanoparticles due to its

expansion during the calcinations process. The sample was dried and calcined at 600 °C. The SEM, TEM images and XRD technique were taken to characterize the α-Fe_2O_3 nanoparticles. The UV-Vis absorption and IR spectra and also TGA results of these samples were documented.

Material and Methods

Starting Materials and Synthesis of α-Fe_2O_3 Nanoparticles: Iron nitrate ($Fe(NO_3)_3.9H_2O$) was purchased from Merck and Gelatin was purchased from Bovine skin, type B, Sigma Aldrich used without further purification. Double distilled water was used to prepare precursor solution. Iron oxide (α-Fe_2O_3) nanoparticles were synthesized by sol-gel method using iron nitrate as iron source and gelatin as polymerizing agent. In a typical synthesis, 4 gm of iron nitrate was dissolved in 100 ml of distilled water and then stirred for 30 min to complete dissolution in the same way we check the pH was approximately 1.4. On the other hand, 1.5 gm of gelatin was dissolved in 100 ml of distilled water and then stirred for 30 min at 60°C in order to get clear solution and the pH was around 5.6. Afterwards, the gelatin solution was added slowly to the iron nitrate solution with stirring. The resulting solution was stirred for an hour and the solution turns to gel followed by drying in hot air oven at 90°C for 6 hours. The obtained compound was calcined at 600°C in air atmosphere for an hour using muffle furnace. In the present work, gelatin was used as a stabilizer and gelling agent for reducing the agglomeration of nanoparticles. Water-soluble gelatin forms a matrix of entangled polymeric chains which includes the cavities that can trap the small volumes of metal ions. The schematic representation of α-Fe_2O_3 preparation by using gelatin solution via sol-gel process is shown in figure 1.

Structural Characterization: The as-synthesized iron oxide (α-Fe_2O_3) compound was subjected to thermogravimetric analysis (TGA) and it was carried out from room temperature to 800 °C under air atmosphere at a heating rate of 5°C/min using a SDTA-85 1e from Mettler Toledo. To determine the crystal phase identification and estimate the crystallite size, X-ray diffraction (XRD) patterns were verified for synthesized samples with Bruker - D8 Advance Powder X-ray diffractometer with Cu Kα radiation, (λCu = 1.5418 Å) working at 30 mA and 40 kV. To measure the particle size and morphology of iron oxide (α-Fe_2O_3) nanoparticles, transmission electron microscopy (TEM), LEO-Libra 120 and scanning electron microscopy (SEM), Zeiss Supra 35VP were used. The FT-IR spectra were obtained at ambient temperature on KBr pellets using the Bruker FT-IR spectrometer (TENSOR 27). FT-IR spectroscopy in the transmission mode gives qualitative information about the way in which the adsorbed molecules are bonded to the surfaces as well as the structural information of solids. The UV–Vis absorption spectra were confirmed by Mettler Toledo spectrometer. For uniform dispersion, the synthesized nanoparticles were dispersed in ethanol and were sonicated prior to UV–Vis measurement.

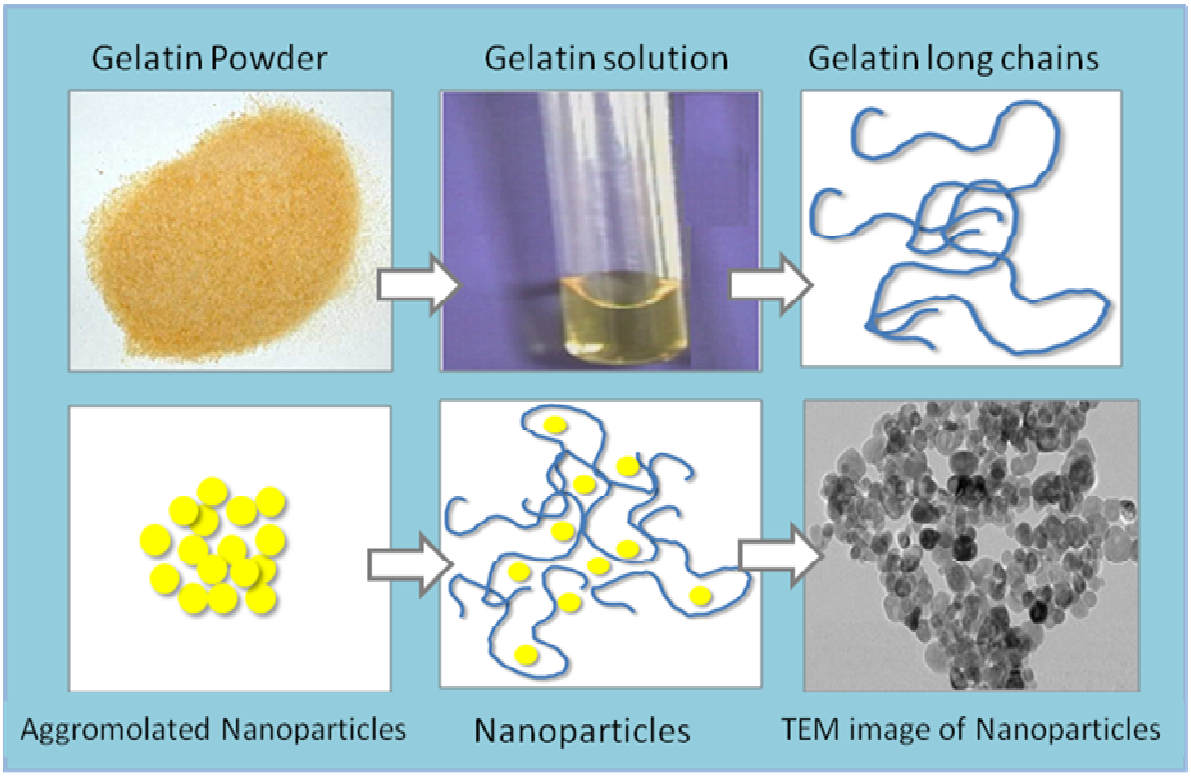

Figure-1
Schematic illustration about the role of gelatin solution to prevents the agglomeration of nanoparticles

Results and Discussion

Powder XRD analysis: The XRD patterns for α-Fe_2O_3 nanoparticles (calcined at 600 °C for 1 hr) prepared by sol-gel process using gelatin as a media and it was illustrated in figure 2. The XRD peaks in the wide angle range of 2θ from 20° to 60° with CuK_α radiation. It can be seen from figure 2, the XRD patterns were indexed to pure hexagonal structure with lattice parameter of a = 5.038(2) Å and c = 13.772(12) Å and its space group: *R*3*c*. The peaks appeared at 2θ range of 24.14°, 33.15°, 35.63°, 40.63°, 49.46°and 54.07° can be attributed to the 012, 104, 110, 113, 024 and 116 crystalline structures corresponds to pure α-Fe_2O_3 nanoparticles. The diffraction peaks are matching with standard JCPDS card no. 87-1164, representing that the α-Fe_2O_3 particles are crystalline structure. By using the Debye - Scherrer equation, the average crystallite sizes were calculated:

$$D = \frac{K\lambda}{\beta\cos\theta} \quad (1)$$

where K is the shape factor (the typical value is 0.89) λ is the wavelength of incident beam, β is the broadening of the diffraction line measured in radians at half of its maximum intensity (FWHM) and θ is the Bragg's angle and D is the diameter of the crystallite size[23]. The (104) plane was chosen to calculate the crystallite size α-Fe_2O_3 nanoparticles. The average crystallite sizes from the XRD data were found to be around 30 nm. No other peaks were observed in calcined compound, which indicates the formation of a pure hexagonal structure of α-Fe_2O_3.

Thermogravimetric (TGA) analysis: The phase formation and decomposition which occurs during heat treatment of precursor compound was confirmed by TGA results. The thermal analysis was carried out from room temperature to 800°C. TGA of an as-prepared compound was performed by heating in air atmosphere at 5°C/min in alumina crucible. Figure 3 shows the thermal analysis (TGA) of precursor compound obtained from sol-gel process by using gelatin solution. It is clear that there are three distinct mass loss steps in the temperature ranges 30°C–140°C, 180°C–450°C and 580°C–650°C, respectively, in TGA curve. The first mass loss is primarily attributed to the evaporation of surface adsorbed water, second mass loss might be volatilization and combustion products of organic species and third one is decomposition of prepared sample. The first weight loss step was gradually around 30°C–140°C. The mass loss was 6.4%, and this loss of weight is ascribed to the removal of surface adsorbed water from aqueous gelatin and nitrate solution. The second step was main mass loss occurred at 180°C – 450°C, and the weight loss was 29.8% which is due to the volatilization and combustible organic products present in as-prepared sample. The third step was minor weight loss occurred in the range of 580°C – 650°C, and this mass loss was 12.5 % which is due to decomposition of synthesized compound. After 650°C the curve illustrates the parallel line with temperature axis representing high stability of α-Fe_2O_3 nanoparticles. There is no associated signal with these latter thermal events in the TGA curve confirming the crystallization and phase transition events of α-Fe_2O_3 nanoparticles.

Electron Microscopic Analysis: The electron photomicrographs of α-Fe_2O_3 nanoparticles achieved from sol-gel derived gelatin media calcined at 600 °C for 1 hr are illustrated in figure 4. Figure 4(a) exposes the SEM images of α-Fe_2O_3 nanoparticles and we examined the particles are well defined and oriented spindle like with small spherical shaped particles. The TEM images of α-Fe_2O_3 nanoparticles obtained from sol-gel process and calcined at 600 °C for 1 hr are shown in figure 4(b). After the heat treatment at 600 °C for 1 hr, the α-Fe_2O_3 particles were found in the range of 30–40 nm. It is clear that α-Fe_2O_3 nanoparticles are mainly present as granules with small and big spherical shaped particles and are well crystallize in nature.

FT-IR spectroscopic studies: The FT-IR spectroscopy was utilized to detect the presence of functional groups adsorbed on the surface of synthesized particles during sol-gel process. Figure 5 shows the FT-IR spectrum of α-Fe_2O_3 powder acquired from sol-gel derived gelatin media calcined at 600°C for 1 hr. According to figure 5, the small absorption peak in the range of 3200–3600 cm^{-1} was observed. This peak was centered at 3476 cm^{-1} corresponds to the stretching vibration of intermolecular hydrogen bond (O–H) existing between the adsorbed water molecules and indicates the lower amount of hydroxyl group. The strong band at 586 cm^{-1} emerging in IR spectrum of calcined (600°C) compound shows the presence of stretching and bending vibrations of the intercalated M–O species. No peak at 2900 cm^{-1} indicating the C – H stretching band, which means all organic compounds are removed from the samples after calcinations at 600°C. The characteristic peak at 586 cm^{-1} becomes very strong, indicating the formation of stretching mode of α-Fe_2O_3. This specifies the occurrence of α-Fe_2O_3 nanoparticles in calcined compounds.

UV–Visible spectroscopic studies: The UV–Vis spectra of α-Fe_2O_3 nanoparticles acquired from sol-gel derived gelatin media and calcined at 600°C for 1 hr were revealed in Figure 6. For recording UV–Vis spectra, the sample of α-Fe_2O_3 solution was prepared by absolute ethanol dispersing by ultrasonic bath. The absorption peak in figure 6 correspond to α-Fe_2O_3 sample calcined at a temperature of 600°C showing the strong absorption in the wavelength of 562 nm. This can be assigned to the intrinsic band gap absorption of α-Fe_2O_3 due to the electron transitions from the valence band to the conduction band[24]. The band gap (Eg) of α-Fe_2O_3 nanoparticles was calculated by utilizing the formula $Eg=hc/\lambda$[25], where c = velocity of light, h = Planck's constant and λ = wavelength. The resultant band gap is 2.2 eV. Additionally, the results of XRD and TEM suggest that the size range of α-Fe_2O_3 particles is around 30–40 nm.

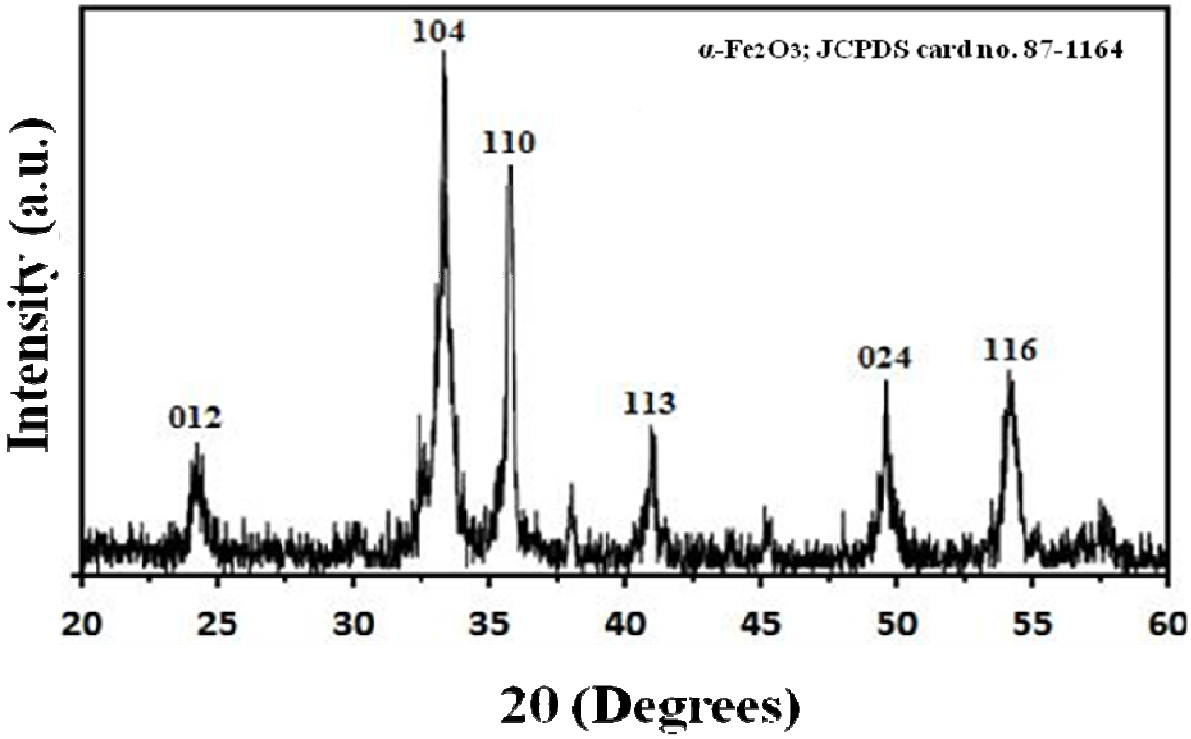

Figure-2
XRD patterns of iron oxide (α-Fe_2O_3) obtained from sol-gel process and calcined at 600 °C for 1 hr

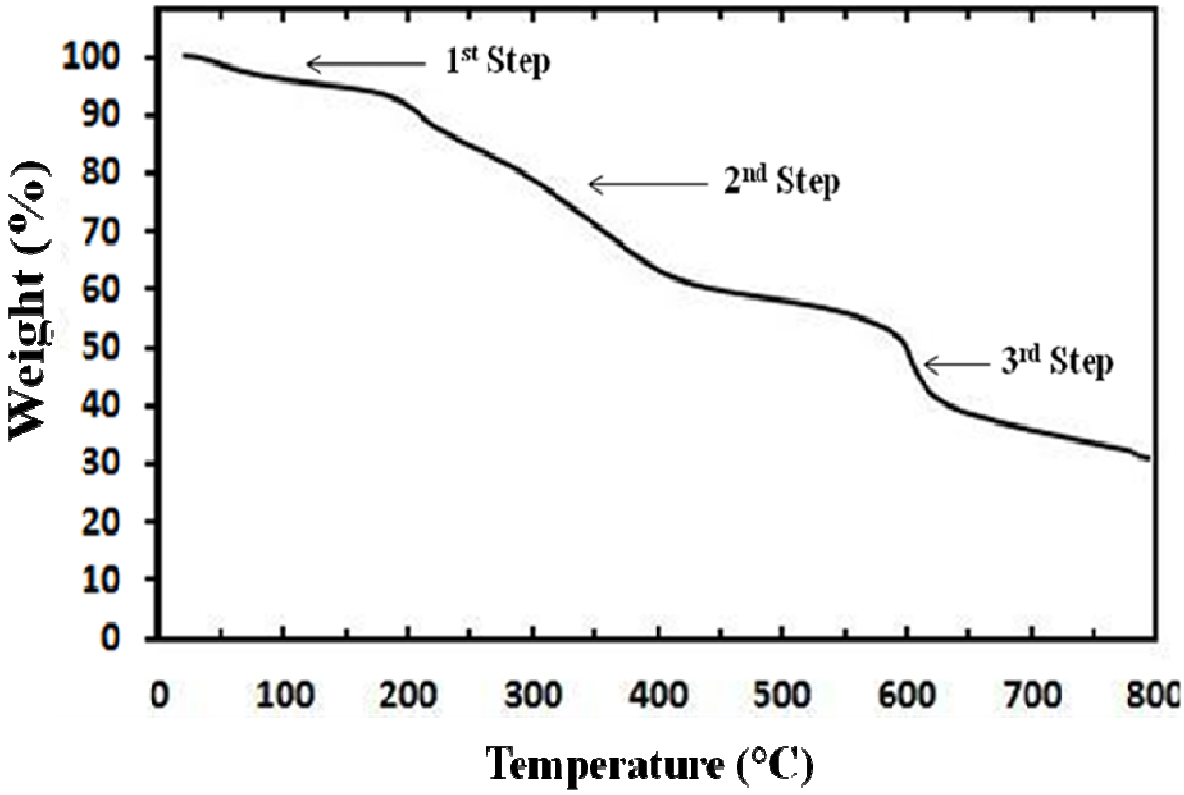

Figure-3
TGA analysis of as-prepared compound obtained from sol-gel process using gelatin media

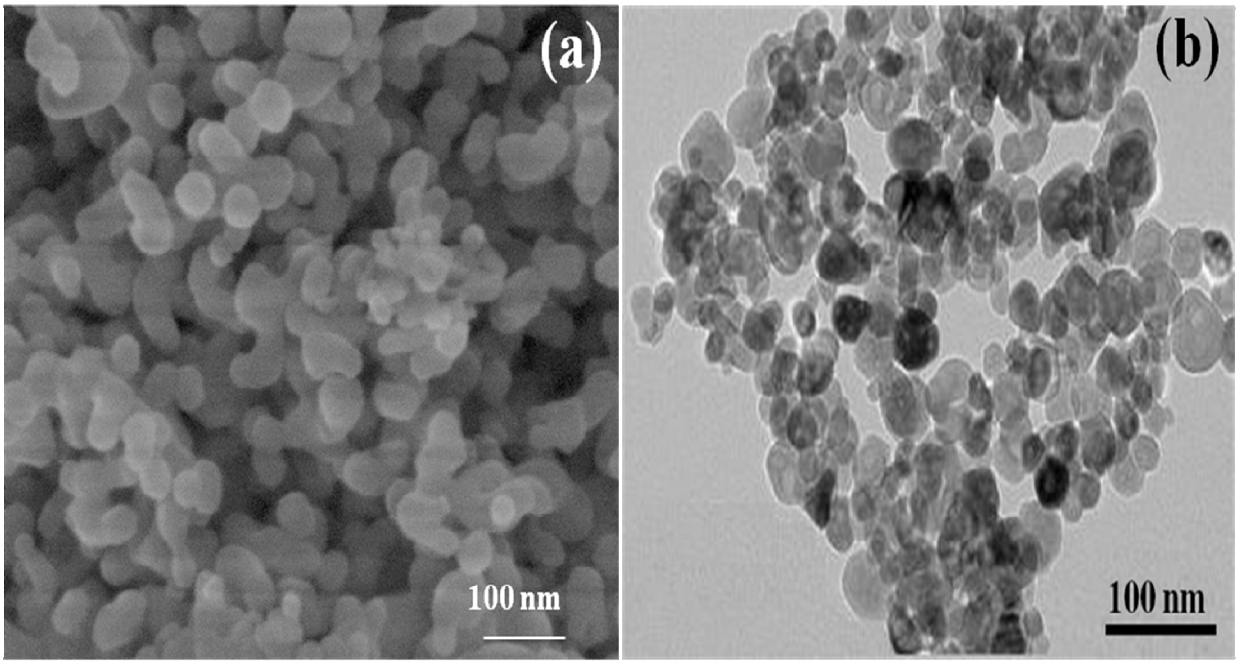

Figure-4
Electron Photomicrographs of α-Fe_2O_3 nanoparticles (a) SEM and (b) TEM image

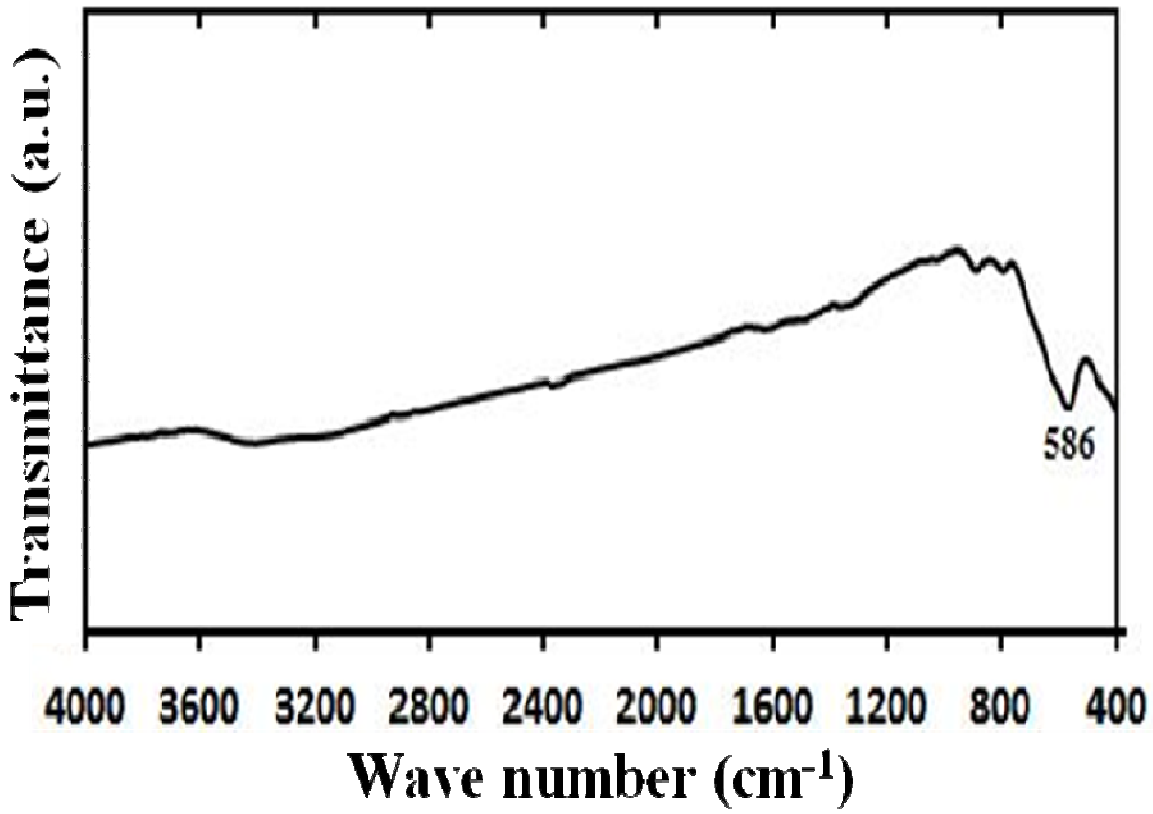

Figure-5
FT-IR spectra of α-Fe_2O_3 obtained from sol-gel process using gelatin media and calcined at 600 °C for 1 hr

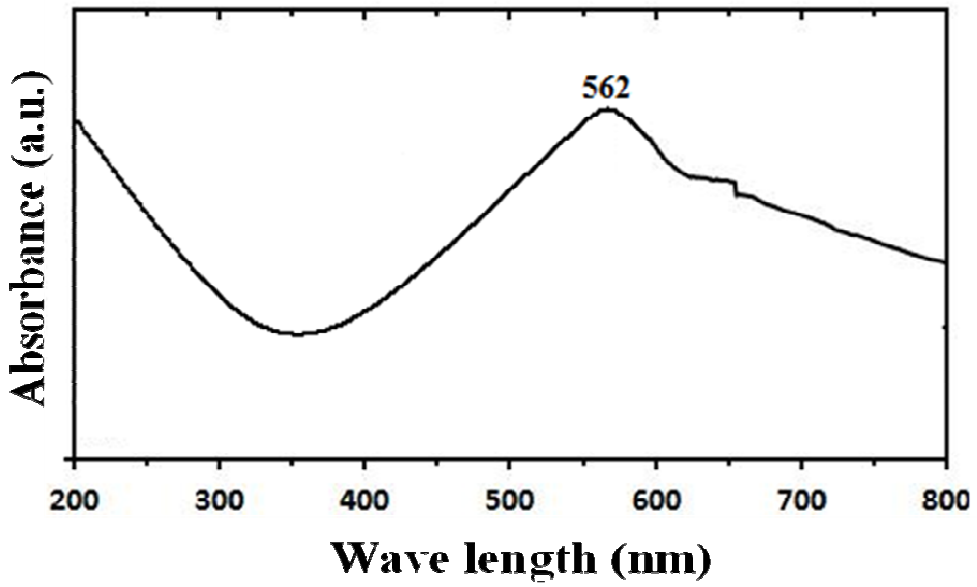

Figure-6

UV–Vis spectra of α-Fe_2O_3 obtained from sol-gel process using gelatin media and calcined at 600 °C for 1 hr

Conclusion

In the present work, the nanosized α-Fe_2O_3 (hematite) particles were synthesized by sol–gel method using gelatin media, successfully. In XRD analysis, the particle size of produced α-Fe_2O_3 was approximately 30–40 nm. TGA revealed that the sample contains CO, NO^-_2, CO_2, and H_2O. The SEM analysis illustrates that the particles morphology was oriented spindle like with small spherical structure. TEM images confirmed the small and big shaped spherical particles and they are highly crystallized in the range of 30–40 nm. The TEM and XRD results indicate that, using gelatin solution as a matrix improves the crystallanity and decreases the size of particles. The FT-IR spectrum demonstrates the existence of small amount of OH^- groups in calcined sample. Gelatin solution forms a matrix of entangled polymeric chains, inside the cavities of which can trap small volumes of metal ions. During heat treatment, the dried precursors decompose into nanocrystalline products. Therefore, the synthesis of α-Fe_2O_3 nanoparticles by sol-gel method is simple and eco-friendly in nature.

Acknowledgment

The authors thank to Nanotechnology and Catalysis research center, University of Malaya, Malaysia for providing lab facilities and this work was supported by the University of Malaya through post doctoral fellowship (HIR grant) and also project grant no. PV-128/2012A.

References

1. Zhang X., Janekhe S.A. and Perlstein J., Nanoscale Size Effects on Photoconductivity of Semiconducting Polymer Thin Films, *Chem. Mater,* **8,** 1571-1574 **(1996)**

2. Fendler J.H., Self-assembled nanostructured materials, *Chem Mat*, **8**, 1616-1624 **(1996)**

3. Madhusudhana N., Yogendra K. and Mahadevan K. M., Photocatalytic Degradation of Violet GL2B Azo dye by using Calcium Aluminate Nanoparticle in presence of Solar light, *Res. J. Chem. Sci.*, **2(5)**, 72-77 **(2012)**

4. Tjong S.C. and Chen H., Nanocrystalline Materials and Coatings, *Mater. Sci. Eng. R,* **45(1-2),** 1-88 (**2004)**

5. Andres R.P., Bielefeld J.D., Henderson J.I., Janes D.B., Kolagunta V.R., Kubiak C.P., Mahoney W.J. and Osifchin R.G., Self-Assembly of a Two-Dimensional Superlattice of Molecularly Linked Metal Clusters, *Science*, **273**, 1690-1693 **(1996)**

6. Kamat P.V., Photochemical and photocatalytic aspects of metal nanoparticles, *J PhysChem B*, **106**, 7729-7744 **(2002)**

7. Perenboom J.A.A.J., Wyder P. and Meier F., Electronic properties of small metallic particles, *Phys Rep*, **78(2)**, 173-292 **(1981)**

8. Pawar M.J., Nimbalkar V.B., Synthesis and phenol degradation activity of Zn and Cr doped TiO_2 Nanoparticles, *Res.J.chem.sci.*, **2(1)**, 32-37 **(2012)**

9. Santhanalakshmi J. and Komalavalli R., Visible Light Induced Photocatalytic Degradation of some Textile Dyes Using Silver Nano Particles, *Res.J.chem.sci.*, **2(4)**, 64-67 **(2012)**

10. Baoliang L.V., Xu Y., Wu D. and Sun Y., Preparation of α-Fe_2O_3 nanodisks by blocking the growth of (001) plane, *J Mater Sci Technol*, **25(2)**, 155-158 **(2009)**

11. Hua J. and Gengsheng J., Hydrothermal synthesis and characterization of monodisperse α-Fe_2O_3 nanoparticles, *Mater Lett*, **63(30)**, 2725-2727 **(2009)**

12. Zhu L.-P., Xiao H.-M. and Fu S.-Y., Template-Free Synthesis of monodispersed and single-crystalline cantaloupe-like Fe_2O_3 superstructures, *Crystal Growth & Design*, **7(2)**, 177–182 **(2007)**

13. Gu J., Li S., Wang E., Li Q., Sun G., Xu R. and Zhang H., Single-crystalline α-Fe_2O_3 with hierarchical structures: Controllable synthesis, formation mechanism and photocatalytic properties, *J Solid State Chem*, **182(5)**, 1265-1272 **(2009)**

14. Jiao F., Harrison A., Jumas J.-C., Chadwick A.V., Kockelmann W. and Bruce P.G., Ordered Mesoporous Fe_2O_3 with Crystalline Walls, *J Am Chem Soc*, **128(16)**, 5468–5474 **(2006)**

15. Tang B., Wang G., Zhuo L., Ge J. and Cui L., Facile Route to α-FeOOH and α-Fe_2O_3 Nanorods and Magnetic Property of α-Fe_2O_3 Nanorods, *Inorg Chem*, **45(13)**, 5196–5200 **(2006)**

16. Chen D.H., Jiao X.L. and Chen D.R., Solvothermal Synthesis of α-Fe_2O_3 Particles with Different Morphologies, *Mater Res Bull*, **36**, 1057-1064 **(2001)**

17. Deb P., Basumallick A., Chatterjee P. and Sengupta S.P., Preparation of α-Fe_2O_3 nanoparticles from a nonaqueous precursor medium, *Scr Mater*, **45**, 341-346 **(2001)**

18. Zhao T., Chen D.H. and Chen D.R., *Chin Chem Lett*, **14**, 323 **(2003)**

19. Xiong Y., Li Z., Li X., Hu B. and Xie Y., Thermally Stable Hematite Hollow Nanowires, *Inorg Chem*, **43**, 6540-6542 **(2004)**

20. Li G.S., Smith R.L., Inomata H. and Arai K., Preparation and magnetization of hematite nanocrystals with amorphous iron oxide layers by hydrothermal conditions, *Mater Res Bull*, **37(5)**, 949-955 **(2002)**

21. Cao M., Liu T., Gao S., Sun G., Wu X., Hu C. and Wang Z.L., Single-Crystal Dendritic Micro-Pines of Magnetic α-Fe_2O_3: Large-Scale Synthesis, Formation Mechanism, And Properties, *Angewandte Chemie International Edition*, **44**, 2-6 **(2005)**

22. Chandrappa K. G. and Venkatesha T. V., Electrochemical bulk synthesis of Fe_3O_4 and a-Fe_2O_3 nanoparticles and its Zn–Co–α–Fe_2O_3 composite thin films for corrosion protection, *Mater. Corr,* **63**, 1-13 **(2012)**

23. He C., Sasaki T., Shimizu Y. and Koshizaki N., Synthesis of ZnO nanoparticles using nanosecond pulsed laser ablation in aqueous media and their self-assembly towards spindle-like ZnO aggregates, *Applied Surface Science*, **254(7)**, 2196–2202 **(2008)**

24. Yu J. and Yu X., Hydrothermal Synthesis and Photocatalytic Activity of Zinc Oxide Hollow Spheres, *Environ. Sci. Technol*, **42(13)**, 4902–4907 **(2008)**

25. Hoffmann M. R., Martin S. T., Choi W. and Bahnemann D. W., Environmental Applications of Semiconductor Photocatalysis, *Chemical Reviews*, **95(1)**, 69-96 **(1995)**